The Journal of Transport and Land Use jtlu.org
Vol. 17 No. 1 [2024] pp. 751–780

JTLU

Analysis of the impact of policy measures on parking behavior using interpretable time series models

Elisabeth Fokker (corresponding author)
Centrum Wiskunde & Informatica
elisabeth.fokker@cwi.nl

Elenna Dugundji
Massachusetts Institute of Technology
elenna_d@mit.edu

Thomas Koch
Massachusetts Institute of Technology
thakoch@mit.edu

Abstract: Growing awareness of the environmental impact of abundant parking has led to recent measures focused on decreasing car use in urban areas. This paper employs interpretable time series models to analyze the effects of these measures on parking demand. The study utilizes a dataset of more than 22 million parking transactions from 3,594 on-street selling points and 8 park-and-ride (P&R) locations in Amsterdam. Three models with external regressors, namely, Error Trend Seasonality (ETSX) models, Seasonal Autoregressive Integrated Moving Average (SARIMAX) models, and Interpretable Multi-Variate Long Short-Term Memory (IMV-LSTM) models, are compared against a Seasonal Naïve benchmark model. The ETSX model achieved the lowest error values, as indicated by both RMSE and SMAPE. The results show a significant decrease in parking (up to a 77% decline), primarily attributed to the tariff change, which had a greater impact than the introduction of a metro line. Moreover, both measures caused a shift in parking to P&R locations and peripheral areas. The introduction of the metro line led to more parking near a new metro station. In addition, COVID-19 measures resulted in a significant decrease in parking demand. These results are presented in an application that visualizes the influence of external regressors on parking ticket demand.

Keywords: Time series forecasting, machine learning, on-street parking, park and ride, interpretable time series models, ETSX, SARIMAX, LSTM

Article history:
Received: November 1, 2023
Received in revised form: April 29, 2024
Accepted: June 12, 2024
Available online: November 1, 2024

1 Introduction

The issue of parking is overlooked by many transportation professionals and urban planners (Kodransky & Hermann, 2011). Nevertheless, it affects the life and accessibility of every active participant in modern society. Whether one is an avid motorist or an everyday cyclist, the impact of parking is embedded in the economy (Shoup, 2005), public space usage (Jakle & Sculle, 2004; Marsden, 2014; Shoup, 2006) and air quality

https://doi.org/10.5198/jtlu.2024.2455
ISSN: 1938-7849 | Licensed under the Creative Commons Attribution – Noncommercial License 4.0

The *Journal of Transport and Land Use* is the official journal of the World Society for Transport and Land Use (WSTLUR) and is published and sponsored by the University of Minnesota Center for Transportation Studies.

(Arnott & Inci, 2006). Growing awareness of these effects has led to changes in parking policies in recent years. Formerly, parking policy was a means to support the increasing car ownership with plentiful parking supply (Jakle & Sculle, 2004; Mukhija & Shoup, 2006). For instance, minimum parking requirements have become a norm in many cities, such as in America (Shoup, 2006), suburban Canada (Engel-Yan et al., 2007), Australia (Taylor, 2020), and later in India, Malaysia, and the Philippines (Barter, 2011). Consequently, the streetscapes of these cities are disrupted by asphalt breaks, blocks of parking garages (Mukhija & Shoup, 2006), and an abundance of parked cars on the streets (Liu et al., 2018). The environmental consequences include the loss of open space and diversity (Mingardo et al., 2015), as well as air pollutants from cruising for parking (Shoup, 2006). As a counter-reaction, parking policymakers strategically focus on reducing car usage in dense urban areas, diverging from the promotion of it.

This objective is accomplished through two key approaches: (1) integrating parking policy into overall urban and transportation policies, and (2) including parking policy as a crucial element of a broader demand management strategy. Recently introduced initiatives include supply restraint (i.e., restricting parking supply), park-and-ride (P&R) facilities (i.e., to facilitate multimodal traveling), dynamic pricing (i.e., differentiated parking fees according to location, time and/or type of vehicle), shared parking (i.e., multiple users share the same parking space, enabling more efficient use of parking facilities) and a workplace parking levy (i.e., a tax imposed on employers who provide off-street private non-residential parking for their staff) (Mingardo et al., 2015).

This paper analyzes the impact of similar changes within Amsterdam, the Netherlands. Just as most European cities (Kirschner & Lanzendorf, 2020), Amsterdam was built before the advent of the car. Due to its high population density, rich mix of functions, and narrow streets, public space is scarce. About 11% of this space is taken up by parked cars. A car spends on average 95% of its time parked (Inci, 2015), with more than 40% of residents' cars remaining stationary on any given day (Van Der Lof & Bussink, 2019). To enhance the livability and accessibility of the city, Amsterdam has launched a plan to reduce car use in the city center, while stimulating public transport, walking, and cycling (Municipality of Amsterdam, 2020). By 2025, 11.2 thousand parking locations will be replaced with pedestrian and bicycle lanes, city parks, and playgrounds. Parking tariffs have increased, car sharing systems are enhanced, P&R supply is expanded, and the public transport network is extended with a new metro line, the North South Line (NSL). To assess the impact of these measures on the demand for parking transaction tickets in on-street parking and P&R facilities, this study proposes interpretable time series models. Interpretability can be defined as “the degree to which a human can understand the cause of a decision” (Miller, 2019). Hence, these models not only predict the target but also assess how the prediction is determined in a human-understandable fashion. The proposed models examine the influence of external regressors on the demand for parking tickets. To compare their performance, the study evaluates the Seasonal Auto-regressive Integrated Moving Average models with exogenous regressors (SARIMAX), Error, Trend, Seasonality models with exogenous regressors (ETSX), and Interpretable Multi-Variate Long Short-Term Memory (IMV-LSTM) models in forecasting the number of parking tickets for the upcoming week, using the Seasonal Naïve model as a benchmark.

The database used in this research includes parking transactions from eight Park and Ride (P&R) facilities and 3,594 selling points. The term “selling point” refers to the location where the transaction occurs to obtain the parking ticket prior to parking. This database, National Parking Register (NPR), is managed by the National Road Traffic Service (RDW) and contains all current parking rights registered on license plate. The target in this research is the number of parking transactions at a given hour between

March 2018 and May 2020. Both forecast and lookback window are 168 hours (i.e., one week). Attributes analyzed include weather, holiday, and event variables, spatial features (i.e., the historic number of parking transactions), the opening of the NSL, parking tariffs, and the intelligent lockdown in the Netherlands due to the COVID-19 pandemic.

This paper is structured as follows: Section two provides an overview of the relevant literature. Section three describes the empirical analysis, followed by the model methodology in section four. Section five examines the performance of the models and analyzes the results from the outperforming model. In section six, we present a decision support system (DSS) that offers interactive visualization of the findings for policymakers. The paper concludes by discussing the findings and offering suggestions for future research.

2 Literature review

Table **1** summarizes the models applied in the relevant literature. The external factors analyzed in these studies are presented in Table 2. From Table 1 it can be noted that Recurrent Neural Network (RNN) models, such as LSTM models and Gated Recurrent Unit (GRU) models are prominent in parking behavior research.

For example, Zhang et al. (2021) introduced a weather-aware LSTM model with event mechanisms for predicting parking behavior. Notably, the model could adapt to events like COVID-19 by utilizing an event module. The authors classified 13 parking locations in China based on their environments, including hotels, commercial streets, shopping malls, industrial parks, markets, and residential areas. The model was trained separately for each environment.

Similarly, Rong et al. (2018) developed an LSTM model to predict real-time parking availability in nine cities across China using sensor data. The model surpassed the baseline models (gradient boosting decision trees and linear interpolation) in various parking categories (apartment, office, mall, food, hospital, park, and entertainment).

Arjona et al. (2020) developed LSTM and GRU models with weather and temporal variables to forecast parking availability in European cities and New York City. The GRU architecture outperformed the LSTM version in most cases, and the inclusion of weather and calendar effects improved predictions for sectors with limited sensor coverage.

In prior studies, Fokker et al. (2021) and Fokker et al. (2022) compared LSTM models with classic time series models (SARIMA, SARIMAX, and ETS) for off-street parking occupancy prediction in Amsterdam, Netherlands. SARIMAX yielded the highest accuracy, with the inclusion of event schedules improving performance by 24%, and the addition of weather variables improving performance by 8%.

Ghosal et al. (2019) combined LSTM models with Convolutional Neural Networks (CNN) to predict block-level parking occupancy. Their approach, called Clustering Augmented Learning Method, learned deep feature representations of spatio-temporal data and simultaneously performed heterogeneous clustering and regression learning. The model, evaluated using San Francisco parking data, outperformed other baseline methods (multi-layer LSTM, LASSO, and historical mean) based on the MAPE metric.

Table 1. Comparison of literature on interpretable time series models in parking behavioral analysis

Research	Prediction target	Dataset	Method*	Metric	Performance outperforming model
Fabusuyi et al. (2014)	Available parking spots	Available parking spaces from garage gates in Pittsburg Downtown area	General regression NN	RMSE, MAE	RMSE: 60.84, MAE: 25.28
Pflügler et al. (2016)	Probability free parking space on a cell in grid	App-collected GPS data in Munich where user presses button if a free parking space is spotted	NN	MSE	16.321
Lu and Liao (2018)	Occupancy rate	On-street block-data at San Fransisco, USA	Naïve Bayes, decision tree	Accuracy	5 hours ahead: 60% – 79%
Rong et al. (2018)	Parking availability	Availability of 2,692 parking lots in Beijing, China and 3,009 parking lots in Shenzen, China	LSTM	Precision, recall	30 min. ahead: precision 0.845 – 0.832, recall 0.844 - 0.831
Camero et al. (2019)	Occupancy rate	Occupancy of 29 car parks in Birmingham	RNN	MAE	6.7 – 10.2
Feng et al. (2019)	Occupancy rate	Occupancy in shopping mall in Ningbo, China	RF, Linear regression, decision tree	RMSE	99 days ahead with daily observations, RF: 0.1662
Ghosal et al. (2019)	Grid-level parking occupancy	San Fransisco on-street parking data (SFpark)	Graph CNN, LSTM	MAE	30 min. ahead: 1.69
Arjona et al. (2020)	Occupancy rate	Occupancy from sensors in indoor and on-street locations in Antwerp, Barcelona, Wattens and Los Angeles	LSTM, GRU	RMSE	6 hours ahead with hourly observations, GRU: 0.089 - 0.120
Provoost et al. (2020)	Occupancy rate	Transaction data of 3 parking garages in Arnhem	NN, RF	MSE, MAE	60 min. ahead, NN: MSE 7.18, MAE 1.87
Fokker et al. (2021)	Absolute occupancy	57 off-street parking locations in Amsterdam, the Netherlands	LSTM, SARIMA, SARIMAX, ETS	RMSE	6 months ahead, SARIMAX: 28.030 – 70.767
Zhang et al. (2021)	Parking arrivals	Arrivals in 13 parking lots in China	LSTM	RMSE	1 hour ahead: 93.84%, 3 hours ahead: 67.54%
This research	Parking arrivals per location zone	Transaction data of 3,594 selling points for on-street parking and 8 P&R locations in Amsterdam	ETSX, SARIMAX, LSTM	RMSE, SMAPE	1 week (168 hours) ahead, ETSX: 3.263 – 32.613 20.540% – 31.342%

* Abbreviations: Long short-term memory (LSTM), Gated Recurrent Units (GRU), Box-Jenkins Seasonal Autoregressive Integrated Moving Average with and without exogenous regressors (SARIMAX and SARIMA, respectively), Error Trend Seasonality models with and without exogenous regressors (ETS and ETSX, respectively), Neural Networks (NN), Convolutional Neural Networks (CNN), Recurrent Neural Networks (RNN)

Another example of deep learning is by Camero et al. (2019). The authors proposed Deep Learning with Recurrent Neural Networks for the task of parking occupancy rate predictions. The model is evaluated using occupancy data from 29 car parks in Birmingham, UK, collected over an eleven-week period.

Other instances of applications include classic neural network (NN) models. For example, Provoost et al. (2020) developed NN models and random forest models to predict the parking occupancy in Arnhem, The Netherlands. In their study, the classic neural network model outperformed the CNN model and random forest models.

Furthermore, Fabusuyi et al. (2014) developed a regression NN model to predict parking space availability in Pittsburgh Downtown garages. The model considered variables such as time of day, rainfall, and snowfall. Time of day (32.47%), rain

(21.45%), and snow (18.67%) were found to be the most influential factors for accurate predictions. The results were presented in a computer and smartphone application.

Table 2. Comparison of external regressors investigated in parking research with interpretable time series models

Research	Time patterns from models	Time patterns from features	Weather	Holiday	Event	Area type	Traffic flow	Parking other locations	Tariff change	Public transport change	COVID-19
Fabusuyi et al. (2014)		×	×		×						
Pflügler et al. (2016)		×	×	×	×	×	×				
Lu and Liao (2018)		×	×	×				×			
Rong et al. (2018)	×	×	×	×	×	×	×				
Camero et al. (2019)		×									
Feng et al. (2019)		×	×	×							
Ghosal et al. (2019)	×	×	×			×	×				
Arjona et al. (2020)	×	×	×	×							
Provoost et al. (2020)		×	×	×	×		×				
Fokker et al. (2021)	×		×	×	×						
Zhang et al. (2021)	×	×	×	×	×	×					×
This research	×		×	×	×	×		×	×	×	×

Pflügler et al. (2016) also applied NN models to predict the probability of an available parking spot per cell in a grid in Munich, Germany. The results indicated that weekday, time of day, location, and temperature significantly affect parking, while events, traffic, vacation time, and rainfall are of secondary importance.

Decision trees are also prominent in parking behavior research. For instance, Lu & Liao (2018) built a decision tree and a Naïve Bayes classifier to predict on-street parking occupancy in San Francisco, USA. Besides temporal variables, the model included spatial features, such as the occupancy of the nearest and most similar parking street blocks. The results obtained surpassed a previous model based on spatiotemporal clustering strategies Richter et al. (2014). Feng et al. (2019) developed decision trees, linear regression models, and a random forest model with temporal and weather variables to predict the parking occupancy in a shopping mall in Ningbo, China. The Random Forest model obtained the lowest errors. The key features included the season, precipitation, and temperature.

These studies suggest that incorporating external regressors is an effective approach not only to enhance model performance but also to provide deeper insights into parking behavior. In the present study, LSTM models with variable interpretability are developed, similar to the papers by Arjona et al. (2020); Fabusuyi et al. (2014); Fokker et al. (2021); Ghosal et al. (2019); Rong et al. (2018); Zhang et al. (2021). Moreover, the ETS models developed in a previous study are enhanced by including external regressors with variable interpretability.

Machine learning models mentioned above are found to be less interpretable compared to classic time series models like SARIMAX, as the information is blended in the hidden states without explicit representation. Further analysis of the advantages and disadvantages of the chosen models is discussed in Section 4.

Table 2 presents the regressors studied in the relevant literature, categorized as structural temporal variables, weather variables, holiday and event variables, spatial variables, and major events. Among these, the most frequently examined factors are temporal variables, which include structural temporal variables, holidays, events, and weather variables. However, limited research exists on the impact of traffic and transportation changes on parking, such as the introduction of a new public transport line or changes in parking tariffs. Previous studies have primarily employed statistical tests (Wang et al., 2020) or probit models (Kelly & Clinch, 2006). This research employs interpretable time series models to investigate the effects of multiple policy changes, addressing gaps in the previous literature. Moreover, to the best of our knowledge, this is the first study to remove external variables and isolate the effects of specific major changes, ensuring homogeneity in the analysis.

3 Data

This study incorporates a dataset of over 22 million parking transactions sourced from 3,594 on-street selling points and 8 P&R locations in Amsterdam, the Netherlands. This proprietary data is provided by the Municipality of Amsterdam and collected by the National Parking Register (NPR). The number of arrivals and the total duration of parking are measured per selling point per hour. The measurement period consists of 792 days, from March 1, 2018, to April 30, 2020. During this time, the NSL was opened on July 22, 2018, and parking tariffs increased on April 14, 2019. The locations of the P&R facilities and the number of selling points per neighborhood and tariff zone are illustrated in Figure 1 and Figure 2, respectively. To ensure clarity for policymakers, the study uses the layout defined by the Municipality of Amsterdam, comprising 80 neighborhoods and 56 tariff zones. The P&R facilities are positioned outside and around the center. Due to the implementation of paid parking regulations throughout central Amsterdam, there is a higher concentration of selling points within the city center compared to the outskirts. Since multiple streets in the old city center are closed to car traffic, fewer selling points can be observed in the heart of the city center.

3.1 Data pre-processing

Figure 3 provides an overview of the applied data preparation steps.

3.1.1 Data cleaning

To identify measurement errors, the Amazon Sagemaker Random Cut Forests algorithm (Guha et al., 2016) is employed for anomaly detection. An anomaly is defined as an observation that deviates from the common pattern observed in the majority of the dataset. These anomalies can manifest as unexpected spikes, breaks in periodicity, or unclassifiable observations.

Because the Random Cut Forests algorithm considers the structure of multiple dimensions, it is well-suited for time series data, which includes an additional time dimension. For example, if parking demand on a Monday at 6 PM deviates from the typical pattern for that specific time, the method detects this as an anomaly, regardless of

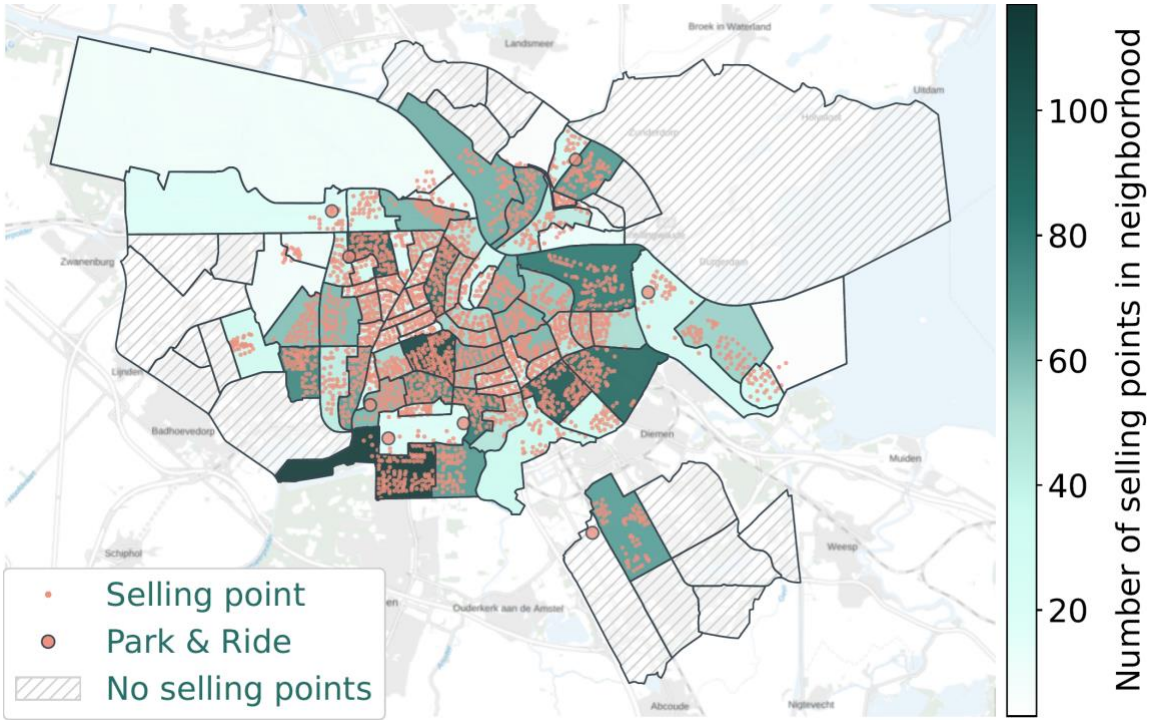

Figure 1. Spatial arrangement selling points per neighborhood and Park and Ride locations

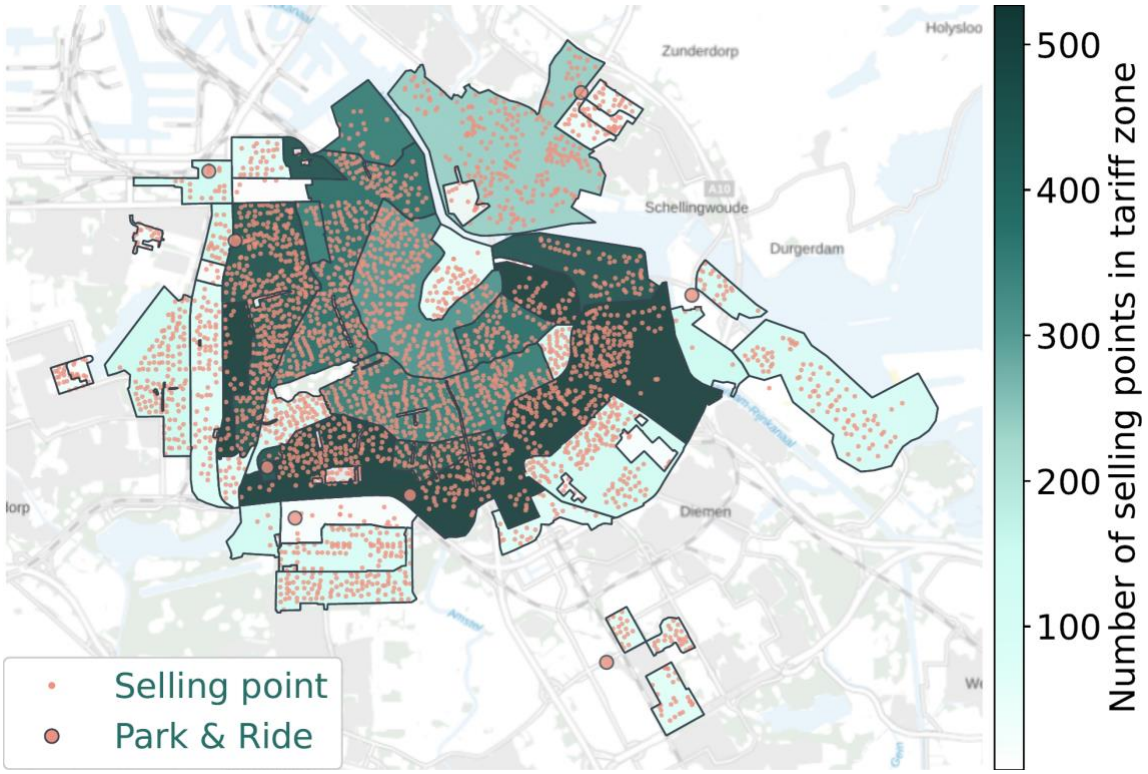

Figure 2. Spatial arrangement of selling points per tariff zone and Park and Ride locations

whether this point differs from the overall parking demand. An anomaly is retained if it occurs during a holiday or scheduled event. Using 1,000 random cut trees, only 0.001% of the NPR observations were identified as anomalies. Subsequently, the removed data points are imputed using Kalman filter imputation (Welsh & Bishop, 1995) in conjunction with a Seasonal Naïve model. A Seasonal Naïve is chosen over more advanced models in this research to avoid favoring one advanced model over another during the training phase.

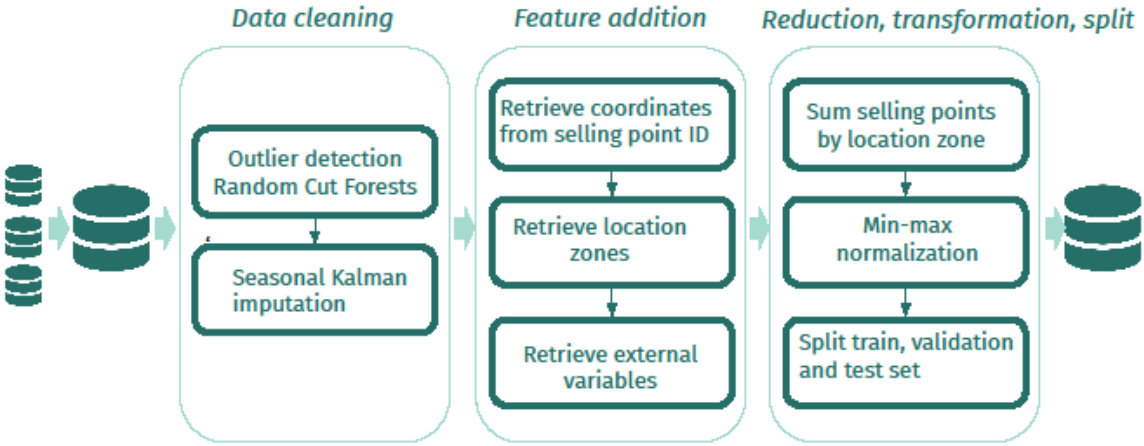

Figure 3. Data pre-processing steps

3.1.2 Feature addition

The coordinates of the selling points are derived from Amsterdam Open Data, allowing for the derivation of location zones at two spatial levels: 56 parking tariff zones and 80 neighborhoods. Each parking tariff zone is governed by distinct parking tariff regulations. The unique parking tariff regulations assigned to each parking tariff zone serve as valuable indicators for evaluating changes in parking behavior resulting from tariff adjustments. Conversely, neighborhoods offer a finer level of granularity, facilitating the exploration of more nuanced details, such as nearby events.

Subsequently, the explanatory variables from Table 3 are retrieved.

Weather attributes. Weather attributes are included in this analysis due to their significant impact on parking behavior, as indicated by various studies (Arjona et al., 2020; Fabusuyi et al., 2014; Feng et al., 2019; Fokker et al., 2021). Weather conditions can influence both the choice of parking location (e.g., a sunny day may lead to increased parking in recreational areas) and the mode choice (e.g., precipitation may result in choosing the car over other modes). The attributes are provided by the Royal Netherlands Meteorological Institute (KNMI) from Schiphol weather station near Amsterdam. These consist of hourly weather observations, such as the sum of precipitation or the average temperature of the previous hour. In the provided selection of weather variables, multicollinearity occurs, i.e., a linear relationship is observed among the independent variables. Therefore, the

weather variables are selected in a way that the variables do not intercorrelate according to the variance inflation factor (Craney & Surles, 2002). This measure is given by

Table 3. Comparison of external regressors investigated in parking research with interpretable time series models

Category	Attribute	Explanation
Weather	Wind speed	Average wind speed (in 0.1 m/s)
	Sunshine	Duration of sunshine (in 0.1 hrs.)
	Precipitation	Sum of precipitation (in 0.1 mm)
Events	Cultural	Number of visitors at a concert, festival or theatre for each location zone for 1, 2, 3, 4 hrs. pre-event, during event, 1, 2, 3, 4 hrs. post-event
	Sports	Number of visitors at a sports event for each location zone for 1-4 hrs. pre-event, during event, 1-4 hrs. post-event
	Meetings	Number of visitors at a conference, convention or trade show for 1-4 hrs. pre-event, during event, 1-4 hrs. post-event
	Traffic closure event	0 = no traffic closure caused by event, 1 = traffic closure caused by event
	Black Friday	0 = no black Friday, 1 = black Friday
Spatial	Arrivals other zones	Number of arrivals in other location zones in the last hour of historic data
Major Changes	Parking addition	0 = pre-addition paid space in zone, 1 = post-addition paid space in zone
Holidays, vacations	Holiday	0 = no holiday, 1 = holiday
	Vacation	0 = no vacation, 1 = vacation
	Parking tariff	Tariff (in €/hr.) in the location zone
	North-South line	0 = pre-NSL, 1 = post-NSL opening
	COVID-19	0 = pre-lockdown, 1 = lockdown

$$VIF_k = \frac{1}{1 - R_k^2}, \tag{1}$$

where R_k^2 is the unadjusted coefficient of determination for regressing the kth independent variable on the remaining ones, defined by

$$\begin{aligned} R_k^2 &= 1 - \frac{\text{sum squared regression } (SSR)}{\text{total sum of squares } (SST)} \\ &= 1 - \frac{\sum(y_k - \hat{y}_k)^2}{\sum(y_k - \bar{y})^2}, \end{aligned} \tag{2}$$

which returns a value between 0 and 1. The value for VIF_k can be interpreted as follows: if $R_k^2 = 0$, the variance of the remaining independent variables cannot be predicted from independent variable k. This then would return $VIF_k = 1$, which means multicollinearity does not exist between the given variable k and the other variables. In this case, the variance of the kth regression coefficient is not inflated. A value between 1 and 5 indicates moderate correlation, while a value greater than 5 indicates high correlation. The final selection had a VIF_k value close to 1 for each independent weather variable k. From these, six weather variables are retained and included as external regressors.

Event attributes. In a previous study (Fokker et al., 2021) it was found that events can have a major impact on the parking demand. Higher parking occupancy near the event venue is observed before and during an event, whereas a decrease in parking occupancy is noticeable after the event. We build upon this concept by including events of three different types: *cultural events*, e.g., concerts, theatre performances and festivals, *sports events*, e.g., soccer matches and *meeting events*, e.g., conferences. The number of visitors has been obtained from open stage schedules, conference schedules and soccer and other sports schedules of various event locations in Amsterdam. By including the number of visitors, instead of indicating whether an event takes place, the model can distinguish between big and small events.

For each event type nine variables are included: 4 to 1 hours before an event, during an event, and 1 to 4 hours after an event. Nine variables are included instead of only one, as the latter would give the false assumption that all visitors arrive and leave at the same time. Instead, visitors arrive and leave gradually before and after an event. Other event attributes added are black Friday and traffic closures, which are dummy variables that explain whether a certain neighborhood has a traffic closure as a result of an event. In total, 722 events took place during the measurement period, of which 429 cultural events, 243 conferences and meetings and 50 sports matches. Finally, 108 event variables are retained (12 different event types by event venue and category, multiplied by 9 variables per event type).

Spatial attributes. Inspired by the paper by Lu and Liao (2018) spatial features are included in the models, defined as the last historic measured number of parking ticket transactions of all other parking locations, except the location of consideration. This expresses the spatial correlations between the parking locations. Spatial correlation can occur, for example, when motorists search for parking. If neighborhood *A* has many arrivals in the last hour, it might result in an increase in arrivals in neighborhood *B* from motorists who could not find a parking place in neighborhood *A*. In the case of neighborhoods, 87 attributes are added to analyze spatial correlation, including 79 other neighborhoods and 8 P&R locations. For tariff zones, 63 features are included, comprising 55 other tariff zones and 8 P&R locations. To take into account selling points that are added later to the transaction data, a dummy variable indicating the time since paid parking started is included. This applies to two neighborhoods in northern Amsterdam where paid parking was previously unavailable, but a tariff has been introduced during the measurement period.

Holidays and vacations. During some public holidays a Sunday rate applies in most of the neighborhoods concerned. In these cases, street parking is often free of charge, resulting in fewer transactions and hence, fewer measurements. Therefore, holidays are added to the models. In addition, school vacations are included, totaling 17 external regressors that indicate the timing of holidays and vacations.

Level shift attributes. Major events can influence the parking behavior in the long term. During the measurement period analogous events are the parking tariff change, the opening of the NSL, and the lockdown in the Netherlands due to the COVID-19 pandemic. The parking tariffs are added for each location, except for the locations where no tariff change took place (which was the case in Amstel III/Bullewijk and the P&R locations). The periods since the opening of the NSL and the start of the lockdown, respectively, are indicated by dummy variables. While other exogenous regressors are analyzed based on the coefficients of the time series models, the impact of the level shift attributes is investigated with another approach, explained in Section 5.2.

3.1.3 Data cleaning

The selling points are grouped by their corresponding location zones. This step reduces the on-street data to 1.53 million records for neighborhood data and 1.07 million records for tariff zone data. A separate predictive model is developed for each zone. This is preferred over a general model because previous work has shown that external regressors can have different effects on parking locations. Moreover, by modeling location zones separately it is possible to investigate spatial differences. Next, the data is scaled using Equation 3

$$y'_t = \frac{y_t - \min(y_t)}{\max(y_t) - \min(y_t)}, \tag{3}$$

where y is the target data, which are the parking arrivals per hour for each location. Finally, the data is split into training, validation and test sets, as visualized in Figure 4. This split is designed to provide sufficient training data for the model to learn post-NSL and post-parking tariff change effects. The model parameters are evaluated on the validation set. The models with the best combination of parameters for each model type are then compared using the test set. Note that the start of the lockdown is excluded from the test set. This is because the start of the lockdown occurs towards the end of the dataset, providing no opportunity for the model to learn from its changes. Therefore, the final outperforming model is applied to the complete dataset, including the last six weeks of measurements during the lockdown.

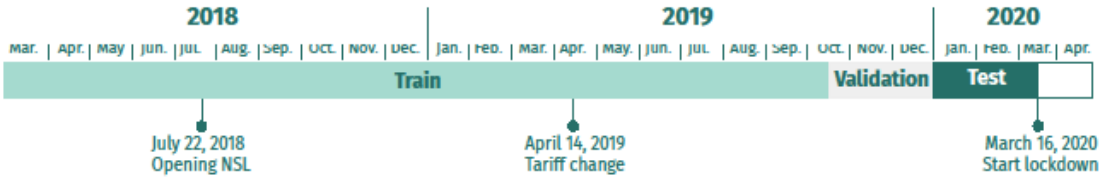

Figure 4. Timeline with the train set, validation set and test set

3.2 Data pre-processing

To visually represent the analysis, focus is directed toward four specific neighborhoods and two P&R locations. The highlighted neighborhoods encompass Buikslotermeer in the north, Burgwallen Nieuwe-Zijde in the center, Zuidas in the south, and Bijlmer Center in the southeast of the city. The selected P&R locations are P&R Bos en Lommer and P&R Olympisch Stadion, chosen because they are the only P&R facilities with available observations prior to the opening of the NSL, providing 24/7 access. P&R Noord and P&R RAI, which are more relevant to the NSL, are excluded from the visualization due to a lack of data in 2018.

Figure 5 presents the correlograms of these locations. The values on the x-axis represent the lag $k \in (0, \dots, 336)$, where 336 equals two weeks (24 hours $*$ 14 days). The values on the y-axis represent the autocorrelation, indicating the correlation of the time series with its shifted variant by k time steps. A distinct peak is observable at every 24th lag from each of the six locations, indicating a 24-hour seasonality. Furthermore, a higher peak is observed at lag 168, signifying a second seasonality of one week. Because

the highest seasonality is one week, a one-week timeframe was chosen for both the forecast and lookback window.

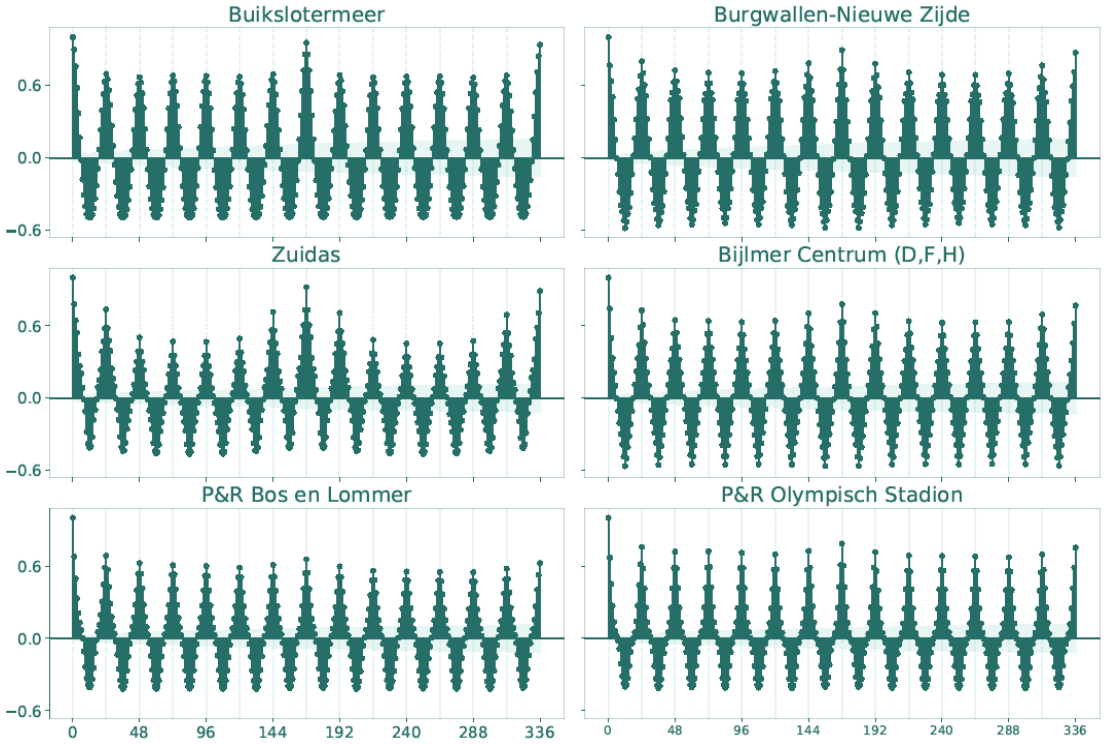

Figure 5. Correlograms of arrivals in six parking locations

4 Model methodology

In this section the time series methods developed in this paper are defined, which are SARIMAX, ETSX and IMV-LSTM models. For each model, the assessment of variable importance for the exogenous regressors with respect to the prediction of the target variable is demonstrated. Considering the deviation from the norm when external regressors come into play, it is crucial for the model to make accurate predictions at these points. For this reason, the models are evaluated using the Root Mean Squared Error (RMSE). This metric is preferred because it penalizes larger deviations more than cumulative small deviations. Its equation is expressed as

$$RMSE = \sqrt{\frac{\sum_{t=1}^{T}(\hat{y}_t - y_t)^2}{T}}. \quad (4)$$

Here, $\hat{y}_t$ denotes the predicted arrivals, y_t represents the actual arrivals, and T stands for the number of time steps in the validation or test set.

To enhance the evaluation process, a supplementary error metric, the Symmetric Mean Absolute Percentage Error (SMAPE), is incorporated. SMAPE provides a balanced assessment by calculating errors symmetrically, thus treating overestimation and underestimation of values equally. This choice is deliberate, as both overestimating and

underestimating parking demand have implications for planning and resource allocation. This equation is given by:

$$SMAPE = \frac{100}{T}\sum_{t=1}^{T}\frac{|\hat{y}_t - y_t|}{|\hat{y}_t| + |y_t|}. \tag{5}$$

Due to the clear seasonal patterns observed in the correlogram (Figure 5), the Seasonal Naïve model was selected as a benchmark approach. This model, while simple and reliant on minimal data manipulation, typically exhibits limitations in accurately predicting highly fluctuating or irregularly influenced data. Furthermore, it is important to note that this model does not include any external regressors. In a Seasonal Naïve model, the forecast value equals the last observed value of this data point from the corresponding season. The model's chosen seasonality is one week, aligning with the highest observed seasonality detected in Figure 5.

4.1 Seasonal ARIMA with exogenous regressors

Given the well-structured nature of the observed data, Seasonal ARIMA models with exogenous regressors (SARIMAX) are a suitable choice for forecasting the number of parking tickets. SARIMAX models have demonstrated their effectiveness in forecasting data with clear seasonal and trend components, as shown in previous studies (e.g., Fokker et al. (2021)). The models offer the advantage of interpretability, thanks to the easily interpretable coefficients of the external regressors. However, SARIMAX models have some drawbacks, including sensitivity to outliers, limited flexibility in capturing nonlinear or non-stationary patterns, and high computational expense during parameter tuning. Therefore, while SARIMAX can be considered a good model for short-term forecasting, it is important to interpret the results with caution and careful consideration.

SARIMAX models are an extension of ARMA models. These combine regression of the past p values of itself (AR(p)) with the weighted mean of the past q error values ε_t (MA(q)). Equation 6 presents this process

$$y_t = \alpha_1 y_{t-1} + \cdots + \alpha_p y_{t-p} + \varepsilon_t + \beta_1 \varepsilon_{t-1} + \cdots + \beta_q \varepsilon_{t-q} \tag{6}$$

where y_t is a stationary time series process, ε_t a white noise process, p the polynomial order of the AR process, q the polynomial order of the MA process, and $\alpha_1 \ldots \alpha_p, \beta_1 \ldots \beta_p$ are estimated from the data. ARMA models assume the time series to be stationary; however, this study deviates from that assumption. The time series under consideration is influenced by both trend and seasonality, causing its values to depend on historical data. To address this, ARMA models can be extended to ARIMA models, which incorporate differencing over the trend with order d. In this context, examples with d equal to 1 and 2 are provided in Equations 7 and 8, respectively.

$$\nabla y_t = y_t - y_{t-1} \tag{7}$$

$$\nabla^2 y_t = y_t - y_{t-1} - (y_{t-1} - y_{t-2}) = y_t - 2y_{t-1} + y_{t-2} \tag{8}$$

A further extension is the SARIMA$(p,d,q)(P,D,Q)$ model, which differences over the seasons of the corresponding parameters p, d, and q. Equation 9 illustrates a first order seasonal difference $D = 1$

$$\nabla_s y_t = y_t - y_{t-s}, \tag{9}$$

where s equals the number of intervals in a seasonal cycle. To extend the model with exogenous regressors, the SARIMA model is combined with a Linear Regression model. The exogenous regressors are added as time series to the final model equation as $\theta_1 x_{1,t} + \cdots + \theta_K x_{K,t}$ with coefficient estimates $\theta_1, \ldots, \theta_k$ for K exogenous regressors (Makridakis et al., 2008). By analyzing the coefficient estimates, one can investigate the impact of each external variable. We propose a stepwise approach to select the model parameters p, d, q, P, D, Q and the exogenous regressors, summarized in Figure 6.

In the initial model all exogenous regressors are included. The polynomial orders p, P, q, and Q are initially set to zero, and d and D are selected based on visual inspection of correlograms. The following steps are repeated until there is no further improvement in RMSE.

Step 1. First, significant exogenous regressors are selected. Considering a significance level of $\alpha = 0.05$, the null hypothesis $\theta_k = 0$ is rejected if the p-value $< \alpha$ for $k = 1, \ldots, K$. Thus, exogenous regressors with a p-value higher than 0.05 are removed from the model.

Step 2. The removed regressors are then stepwise added to the model, which can potentially be significant when added in a different combination and order.

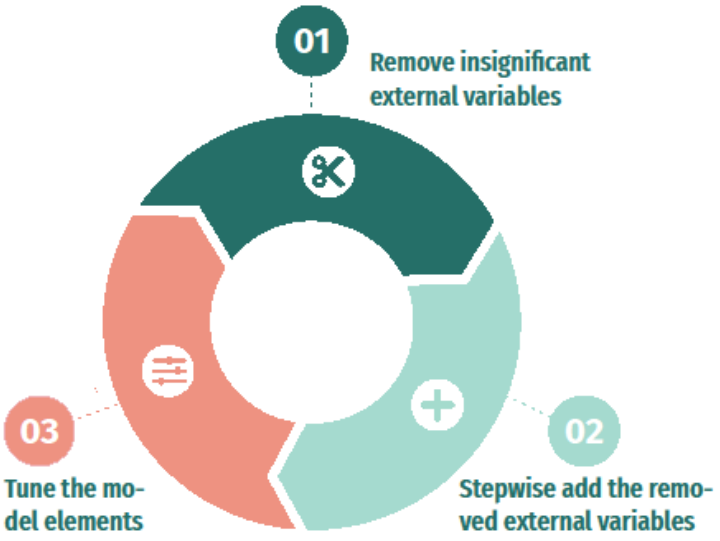

Figure 6. Three-step method for tuning SARIMAX models

Step 3. The polynomial orders p, P, q, and Q are tuned using the Hill-climbing algorithm (Russell & Norvig, 2016). This method is computationally efficient compared to more rigorous approaches (e.g., grid search) and guarantees a local optimum. Based on a test on 10 random locations where the model parameters are selected with grid search, we found that both algorithms obtained the same results. However, the 3-step approach using the Hill-climbing algorithm was on average 10 times faster.

4.2 ETSX

An observed time series can be decomposed into three components: an error, a trend and seasonality. Standard ETS models apply different variants of exponential smoothing based on the combination of component types (Hyndman et al., 2008). The type of error can be additive or multiplicative; the trend can be constant, linear, damped, or exponential; and the seasonality is either additive, multiplicative, or non-existent. The ETSX model improves forecasting performance by coupling an ETS model with explanatory variables (Bisht & Ram, 2021). Equations 10 and 11 formulate the ETSX model for time series with additive and multiplicative error types, respectively.

$$y_t = \theta_t + \theta_1 x_{1,t} + \theta_2 x_{2,t} + \cdots + \theta_K x_{K,t} + \varepsilon_t, \tag{10}$$

$$\nabla^2 y_t = y_t - y_{t-1} - (y_{t-1} - y_{t-2}) = y_t - 2y_{t-1} + y_{t-2}, \tag{11}$$

where θ_0 is the estimated value determined by the ETS components, $x_{k,t}$ is the kth explanatory variable, θ_k is the parameter for that component and K is the number of external regressors. The estimated parameters $\hat{\theta}_k$ are obtained during the optimization stage using the branch and bound algorithm. In general, ETSX is a regression model with time varying intercept, defined by the ETS components and smoothing parameters. ETSX models, similar to SARIMAX models, effectively capture changing patterns and seasonality, as demonstrated in this study. They provide interpretability and transparency, and their forecasting accuracy is enhanced by incorporating exogenous variables. However, ETSX models face challenges similar to SARIMAX models, such as limited handling of complex dependencies and non-linear relationships, the assumption of stationary data requiring preprocessing for non-stationary series, as well as sensitivity to outliers and missing values. When applying ETSX models, it is crucial to consider these factors and select the modeling approach that aligns with the specific characteristics and requirements of the forecasting task. Given the well-structured nature of the data in this research, it is anticipated that ETSX models would be a suitable choice. In contrast to SARIMAX models, the selection of exogenous regressors in ETSX models is not based on statistical tests but on the AICc (Akaike information criterion with a correction for small sample sizes). The external regressors are selected in the following steps.

1. First, an ETS model with only the constant and target variable is constructed.
2. The correlations between the residuals of the model and all external regressors not yet in the model are calculated. A high correlation indicates that a part of the error can be explained by one of the external regressors.
3. The external variable with the highest correlation is added to the model.
4. The AICc is calculated. If this results in a model with a higher AICc, the process is repeated from step 2. Otherwise, the external variable is not added to the model.

The intuition behind this approach is that if the residuals can be explained by an external variable, the model is not yet complete, and this external variable should be added to the model.

4.3 Interpretable multi-variate LSTM

Literature has shown that LSTM models are a powerful method for predicting parking behavior (Arjona et al., 2020; Fokker et al., 2021; Zhang et al., 2021) due to their capability to capture long-term dependencies and model intricate patterns. LSTM is an RNN architecture used in deep learning. A standard RNN model can be described as a chain of neural networks. By chaining neural networks up, a sense of memory is added which allows to identify correlations and patterns in sequential data, such as time series. Nonetheless, exploding and vanishing gradients occur when calculating the gradient. This prevents the standard RNN model from learning long-term dependencies. Exploding gradients can be resolved with gradient clipping; however, solving the vanishing gradient problem is a bigger challenge. To this end, Hochreiter and Schmidhuber (1997) designed a new RNN architecture, the LSTM model. The main idea of LSTM is that the model now has a cell state c_t that passes forward information through the complete chain with only minor interactions. This adds a long-term memory to the model. Gates —a forget gate $\mathbf{f}_t$, an input gate $\mathbf{i}_t$, and an output gate $\mathbf{o}_t$ at time t —carefully regulate which information is passed forward to this cell state. However, LSTM models also present challenges, including (1) their increased complexity compared to traditional feed-forward neural networks, making them harder to understand and train; (2) the potential for overfitting, particularly when working with limited data; and (3) their computationally expensive nature when training and deploying, attributed to larger hidden layer sizes or complex architectures. Moreover, since LSTM models blend the information of the variables into the hidden states, the contribution of each individual variable to the target is intractable. In order to investigate variable importance and variable-wise temporal importance, Guo et al. (2019) have explored Interpretable Multi-Variate LSTM (IMV-LSTM) models. We build our models from their architecture. To be consistent with their work, IMV-LSTM hidden state and gate matrices are denoted with a tilde (~). Then, the hidden state update is defined in

$$\tilde{\mathbf{j}}_t = \tanh(\boldsymbol{\mathcal{W}}_j \otimes \tilde{\boldsymbol{h}}_{t-1} + \boldsymbol{\mathcal{U}}_j \otimes \mathbf{x}_t + \mathbf{b}_j) \tag{12}$$

where $\boldsymbol{\mathcal{W}}_j$ is the weight matrix of the activation value of the previous time step, $\tilde{\boldsymbol{h}}_{t-1}$ is the activation value of the previous time step, $\boldsymbol{\mathcal{U}}_j$ is the weight matrix of the new input, $\mathbf{x}_t$ is the new input and $\mathbf{b}_j$ is a bias vector. Here, $\tilde{\mathbf{j}}_t$ denotes the cell input activation vector.

With the tensor-dot operation $\otimes$ the product of two tensors among the axis of the exogenous regressors is taken. In this fashion, each element of the hidden matrix covers information exclusively from a single input variable. This enables later retrieval of variable-wise importance. The forget gate, input gate and output gate are presented in Equations 13, 14, and 15, respectively.

$$\tilde{\mathbf{f}}_t = \sigma(\boldsymbol{\mathcal{W}}_{\tilde{\mathrm{f}}} \otimes \tilde{\boldsymbol{h}}_{t-1} + \boldsymbol{\mathcal{U}}_{\tilde{\mathrm{f}}} \otimes \mathbf{x}_t + \mathbf{b}_{\tilde{\mathrm{f}}}) \tag{13}$$

$$\tilde{\mathbf{i}}_t = \sigma(\boldsymbol{\mathcal{W}}_{\tilde{\mathrm{i}}} \otimes \tilde{\boldsymbol{h}}_{t-1} + \boldsymbol{\mathcal{U}}_{\tilde{\mathrm{i}}} \otimes \mathbf{x}_t + \mathbf{b}_{\tilde{\mathrm{i}}}) \tag{14}$$

$$\tilde{\mathbf{o}}_t = \sigma(\boldsymbol{\mathcal{W}}_{\tilde{o}} \otimes \widetilde{\boldsymbol{h}}_{t-1} + \boldsymbol{\mathcal{U}}_{\tilde{o}} \otimes \mathbf{x}_t + \mathbf{b}_{\tilde{o}}) \tag{15}$$

Then the update of the cell is given in Equation 16 and the hidden update in Equation 17.

$$\tilde{\mathbf{c}}_t = \tilde{\mathbf{f}}_t \odot \tilde{\mathbf{c}}_{t-1} + \tilde{\mathbf{i}}_t \odot \tilde{\mathbf{j}}_t \tag{16}$$

$$\widetilde{\boldsymbol{h}}_t = \tilde{\mathbf{o}}_t \odot \tanh(\tilde{\mathbf{c}}_t) \tag{17}$$

where $\tilde{o}_t$ is a tensor-dot operation, causing the gates and memory cells to be matrices as well. After running the model, a sequence of hidden state matrices $\widetilde{\boldsymbol{h}}_1, \dots, \widetilde{\boldsymbol{h}}_T$ and the sequences of hidden states of a specific variable n is then $h_1^n, \dots, h_T^n$. Then, a mixture attention mechanism is developed to retrieve the variable and temporal relevance from the hidden state matrices.

In the current study the following selection of external regressors are compared using the RMSE: significant exogenous regressors according to ETSX and SARIMAX, all external regressors, and no external regressors. The selections according to ETSX and SARIMAX obtained similar results, while including all variables and using no variables resulted in higher RMSE values. The hyperparameters of each model, with the best selection of exogenous variables, are trained using a multivariate Tree-structured Parzen Estimator from the Optuna framework (Akiba et al., 2019). By employing the search spaces in Table 4, the model with the lowest RMSE for the parking location of consideration is selected.

Table 4. Search space for tuning IMV-LSTM using Optuna

Hyperparameter	Explanation	Distribution	Search space
Learning rate	Controls parameter updates, impacting learning speed with learning rate times gamma.	Log-uniform	[1e-6, 1e-1]
Step size	Number of time steps processed at each iteration.	Discrete uniform	5, 20, ..., 80, 95
Gamma	Weight for LSTM gate updates.	Uniform	[0.1, 0.9]
Batch size	Number of samples processed in one iteration.	Discrete uniform	24, 48, ..., 168, 192
Size hidden layer	Number of LSTM units in the hidden layer.	Discrete uniform	4, 8, 16, 32, 64, 128, 256

5 Results

5.1 Comparison of models

Before delving into the comparative analysis of our models and their performance indicators, the effectiveness of the models has been evaluated. In evaluating each model, we considered the following key factors. Firstly, we examined their ability to accurately account for event-driven influences, such as fluctuations in parking demand during specific periods. Secondly, we assessed their durability in outlier scenarios, particularly during significant events, to measure their robustness in handling unexpected disruptions to parking patterns. Lastly, we analyzed the integration of external variables into the

models to enhance prediction precision and capture nuanced variations in parking demand dynamics. The selection of models for this study was based on their suitability for handling various types of parking demand data. SARIMAX is particularly proficient at forecasting data characterized by distinct seasonal and trend components, facilitated by its utilization of easily interpretable coefficients of external regressors. In contrast, ETSX integrates exponential smoothing with explanatory variables, thereby augmenting forecasting accuracy through the inclusion of exogenous factors. Lastly, IMV-LSTM excels in capturing long-term dependencies and complex patterns in the data. Its multivariate nature enables the assessment of the effects of external variables on the target variable, thereby enhancing its predictive capabilities and interpretability. Since clear seasonal patterns in real-world parking demand have been noted (see Figure 5), it is expected that models equipped to capture seasonal components, such as ETSX and SARIMAX, would exhibit strong performance. Conversely, in scenarios where parking demand demonstrates high volatility, IMV-LSTM may emerge as a preferable option. Seasonal Naïve model is expected to underperform due to its inherent limitations in capturing outliers and external variables.

Figure 7 compares the prediction performance of the models against the actual values in neighborhood Bijlmer Center from Monday February 24 to Sunday March 2, 2020. Throughout the week, events occurred on Thursday, Friday, and Sunday.

The final RMSE and SMAPE values are presented in

Table **5**. It can be observed that, for the six locations and both error metrics, the ETSX model obtained the lowest error results. This model was also the outperforming model for most of the other locations. One reason for this is that ETSX used external variables to improve the target prediction, making it more capable of accurately predicting events. The second-best model in the highlighted locations is SARIMAX, and sometimes IMV-LSTM. The errors of both models are still well below the errors of the Seasonal Naïve model. This underscores the importance of incorporating external regressors for accurate predictions, especially in the case of outliers that fall outside the structural time patterns, such as events. When comparing the ETSX and SARIMAX models, it can be observed that the only point where ETSX models consistently perform better than SARIMAX models is one week after an inaccurately predicted spike, such as a major event. The models experience relatively large errors at times due to the significant variability in the number of arrivals. Meanwhile, SARIMAX models typically have a higher smoothing factor for seasonality compared to ETSX models, resulting in a more prominent incorporation of errors in predicting the target for the next week.

5.2 Analysis of exogenous regressors

Figure 8 – Figure 11 illustrate the impact of the level shift attributes “North-South Line,” “Parking tariff,” and “COVID-19” on the parking demand in the examined on-street location zones and P&R locations, using the results from the ETSX model.

From Figure 8 it can be noted that in most neighborhoods no significant impact of NSL was measured. However, with the metro line's opening, parking demand in the north has increased by 81%. Given the proximity to the NSL's North station, travelers in this neighborhood are likely to opt for the metro for their onward journey. Moreover, a negative impact can be observed in the east of Amsterdam (up to -77%) and in P&R Olympisch Stadion. Possibly, commuters who previously parked at these locations found a better alternative since the opening of the NSL. Figure 9 visualizes the percentage decrease in parking demand as a result of the COVID-19 lockdown in the Netherlands. In almost every location a strong impact is detected. The most substantial reduction is observed at P&R locations in the South of Amsterdam, with a peak of up to 100% at P&R RAI, which was closed during the lockdown. Additionally, a reduction is observed at Business Park Sloterdijk in Amsterdam North-East. These outcomes are expected due

to the high business density in these areas, combined with the recommendation to work from home. Figure 10 and Figure 11 demonstrate the impact of parking tariff increase on neighborhood level and tariff zone level. From the figures, it can be identified that the parking tariff change had the desired effect: significantly less motorists park in the more expensive dense, central areas (until -22%), while an increase is found in the peripheral zones and P&R locations. An increase in parking ticket demand is detected in the East, where parking tariff increase has been set from €1.40 to €2.50, which is less costly than its neighboring, more central areas (€4.50).

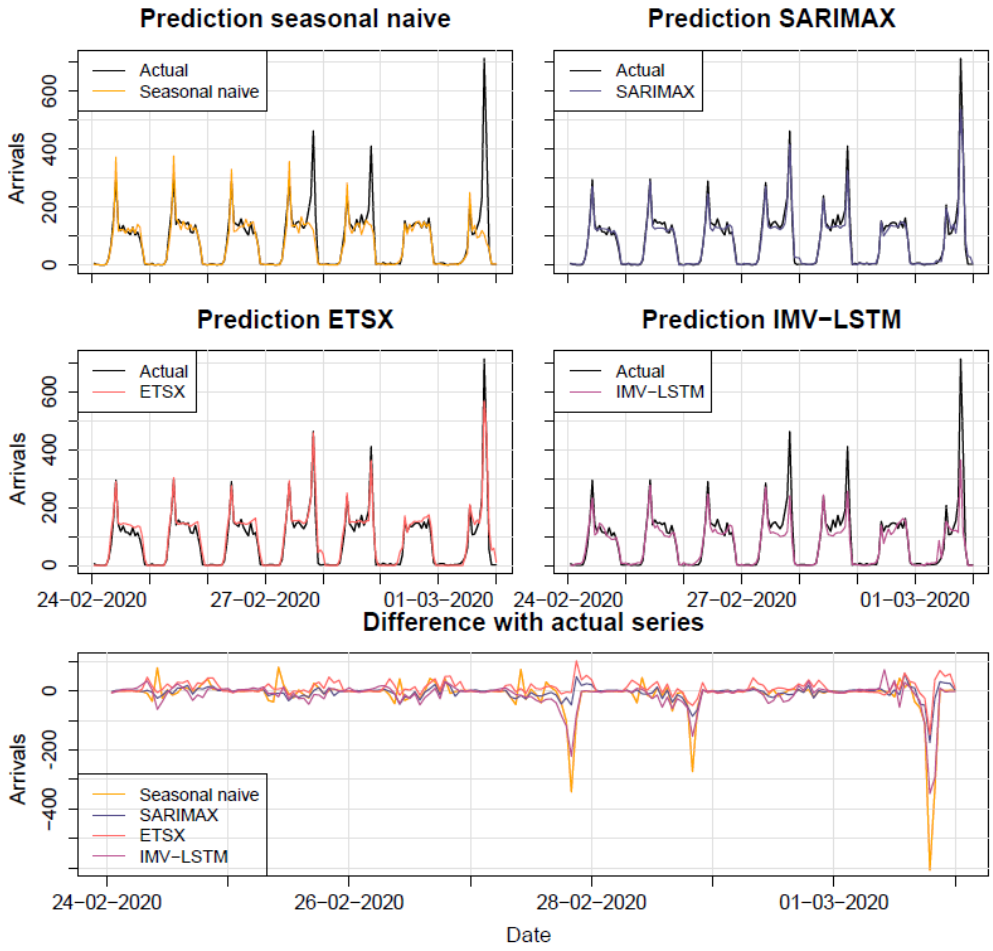

Figure 7. Comparison of predicted versus actual results in Bijlmer Center between February 24 until March 2, 2020

The six locations mentioned in Section 3.2 are analyzed in more detail. The percentage impact of an external variable, denoted as δ_k with $k \in \{1, \dots, K\}$, on parking demand in a specific location is quantified by Equation 18.

$$\delta_k = \frac{\theta_k}{\frac{1}{T}\sum_{t=1}^{T}(y_t - \sum_{\bar{k}=1}^{K}\theta_{\bar{k}} * x_{\bar{k},t})} * 100\%. \tag{18}$$

Table 5. RMSE and SMAPE comparison between the models for on-street parking locations and P&R facilities

	Metric	Buikslotermeer	Burgwallen-Nieuwe zijde	Zuidas	Bijlmer Center	P&R Bos & Lommer	P&R Olympisch stadion
Seasonal Naïve	RMSE	58.139	9.293	14.168	57.771	4.692	6.714
	SMAPE	47.909%	49.548%	37.886%	55.650%	52.260%	54.917%
SARIMAX	RMSE	36.311	6.736	10.292	29.261	3.455	5.743
	SMAPE	28.505%	20.949%	31.559%	23.179%	30.951%	27.228%
ETSX	RMSE	**32.613**	**6.570**	**9.796**	**24.329**	**3.263**	**5.076**
	SMAPE	**24.354%**	**20.540%**	**31.342%**	**21.252%**	**26.887%**	**22.914%**
IMV-LSTM	RMSE	42.709	7.946	12.394	42.247	4.125	5.232
	SMAPE	34.872%	23.032%	36.390%	30.946%	38.786%	24.532%

Here, θ_k denotes the coefficient associated with the kth external variable, T represents the total number of time steps, y_t signifies the number of parking transactions at time t, $\theta_{\bar{k}}$ is the coefficient corresponding to the external variable at time t, and $x_{\bar{k},t}$ denotes the value of the external variable at time t. Intuitively, the coefficient value is normalized by dividing it by the overall mean of the time series after removing exogenous regressors. This normalized value is then scaled by 100% for interpretability. The parameter δ_k signifies the alternation in the time series when regressor k is incorporated, in contrast to the scenario where no external factors are considered.

Table 6 presents the impact of the exogenous regressors on the parking demand (in %) for the six locations. Insignificant variables are marked with a "-". From the weather attribute results it can be observed that wind speed, temperature and sunshine result in slightly less motorists to park at the locations. Thunderstorm has a larger impact on the parking behavior with 4.14% less parking demand in P&R Olympisch Stadion. Precipitation and view have a positive effect on parking, because this may cause the motorist to choose the private car over another mode.

Because the cultural, sports and meeting events are in % change per visitor, the values are lower. In general, sports events result in more motorists to park on-street in Bijlmer Center where the stadium is located, but also affect other locations, such as P&R Bos en Lommer. More motorists tend to park in the center (Burgwallen-Nieuwe Zijde) during cultural events. The impact of meeting events varies per parking location. Because of the high amount of significant event variables, the hours before and after the event are not included in the table.

Holidays and vacations greatly impact parking behavior. For instance, New Year's Eve sees a significant decrease in parking (65.5% less in Buitenveldert). Similarly, King's Day shows a substantial impact (e.g., a 100% decrease in P&R Olympisch Stadion). This can be attributed to free parking on these national holidays, leading to fewer transactions.

Spatial features can be explained as follows: Taking the example of the Zuidas (ZUI) column, the value of 0.39 at Business terrain Sloterdijk (Business Slo.) indicates that there is a 0.39% increase in car parking at Zuidas per arrival in Business terrain Sloterdijk one hour prior. Notably, the parking behavior in one location is not necessarily affected by the arrivals of a neighboring location, but more often by the arrival's locations further away. For instance, one arrival in Grachtengordel Zuid in the past hour

does not affect neighboring Burgwallen Nieuwe-Zijde (BUR), but results in 0.09% more travelers to park in Bijlmer Center (BIJ) in the South East of Amsterdam.

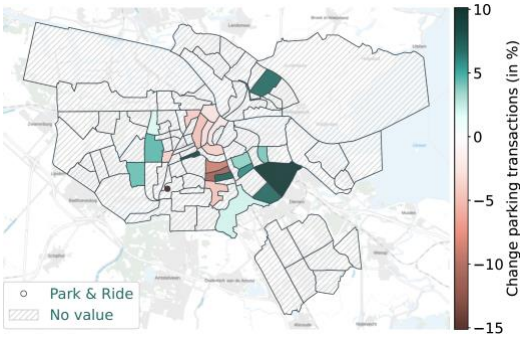

Figure 8. Percentage change due to North-South line

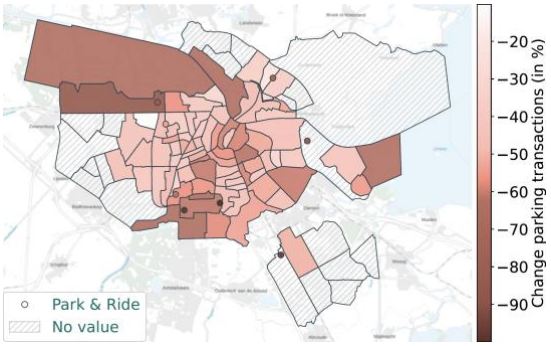

Figure 9. Percentage change due the COVID-19 measures

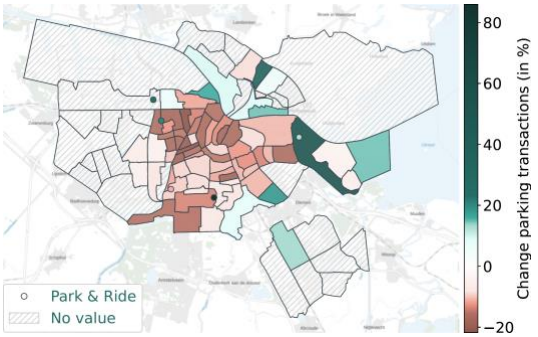

Figure 10. Percentage change due to the tariff increase, neighborhoods

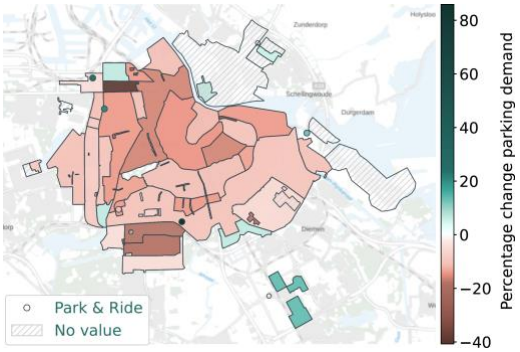

Figure 11. Percentage change due to the tariff increase, tariff zones

Finally, the level shift attributes lead to a significant change in parking ticket transactions. All six locations are affected by the parking tariff change, particularly those with a higher rate increase like Burgwallen-Nieuwe Zijde and Zuidas, resulting in a reduction of over 13% in parkers. On the other hand, P&R Bos and Lommer and Bijlmer Center, where no parking rate increase is found, experienced an increase in demand of 20.3% and 13.4%, respectively. The NSL has caused less travelers to park in the center (e.g., 2.47%) and the P&R locations (11.1% and 15.1%). The P&R locations of consideration are not located nearby the metro stations of the NSL. Possibly, travelers who previously parked at these locations found a better alternative in P&R Noord or P&R RAI. In Buitenveldert an increase of 7.02% is found after the opening of the NSL. In all six locations, COVID-19 resulted in significantly less (37.2% to 61.3%) parking transactions. The impact of the level shifts is also visually presented in Figure 12. This Figure illustrates the week averages of the time series with the exogenous variables removed, retaining only the trends in the data for a neighborhood in the city center. It can be noted that in the center a decrease occurred after the opening of the NSL. This decrease is even stronger as a result of the parking rate increase. Finally, the COVID-19

measures have caused a huge drop. From this, we can conclude that the measures have had an effect in reducing the number of street parking in the city center.

Table 6. Percentage change in parking demand caused by exogenous regressors for six parking locations

Type	Attribute	BUI*	BUR	ZUI	BIJ	PRB	PRO	Attribute	BUI	BUR	ZUI	BIJ	PRB	PRO
Weather	Wind speed	-	-0.02	-	-	-	-	Precipitation	-	-	0.02	-	-	-
	Temperature	-0.04	-	-0.10	-	-	-	Thunderstorm	-	-	-	-	-	-4.14
	Sunshine	-0.10	-0.09	-0.17	-	-0.81	-0.18	View	0.02	-	0.11	-	-	-
Events**	Cult Amstel	-	4e-5	-	-2e-4	-	-	Sport Amstel	-	-	-	1e-6	2e-4	-
	Cult Weesper.	-	5e-3	-	-	-0.02	-	Meet Jordaan	-	-	-	-	-	0.02
	Cult Zuidas	-3e-4	2e-3	-	-	-3e-3	-	Meet Zuidas	-	-1e4	-	-	6e-4	-
	Cult IJplein.	-	-	-	-	-	-0.01	Meet IJplein.	-	-	-	-	-	-0.02
	Cult De Weter.	-	1e-4	-	-	-0.01	-0.01	Meet Burg.-O.	-	2e-3	-	-	-	-
	Dam Run	-	-	-	-	-	-	Pride Fests	-	-	25.5	-	39.2	-
	Pride Walk	-13.3	-	-	-	-	-	Canal Pride	19.4	-8.5	-	-	-	-
Holiday,	Easter Mon.	-	-	-	-	-	29.7	May Break	-	-	-	-	-	10.9
vacation	King's Day	-	-	-9.09	-	-	-100	Autumn break	-	2.5	-	-	-	-
	New Years Eve	-65.8	-	-4.19	-	-	-28.4	Christmas br.	-	-6.3	5.94	-	-	-
Spatial	Business Slo.	-	-	0.39	-	0.15	-	Prinses Irene.	-	-	-	-	0.17	-
	Buiksloterm.	-	0.03	-	-	-	-	Sloterdijk	-	-	0.36	-	-	-
	Buitenvel.-O.	-	-	-0.19	0.14	-	-	Slotermeer-N.	-	0.02	-	-	-	-
	Burg.-O.	0.10	-	-	-	-	-	Slotermeer-Z.	-	-	-	-	-	0.17
	Centrale M.	-0.02	-	-	-	-	-	Slotervaart N.	-	-	0.37	-	-	-
	Chassébuurt	-	0.19	-	-	-	-	Westelijk Ha.	-0.06	-	-0.37	-	-	-
	Dapperbuurt	-	-	-	-	-0.17	-	Westlandgra.	-	-0.19	-	-	-	-
	Grachteng.-Z.	-	-	-	0.09	-	-	Willemspark	-	-	-	-	-0.21	-
	Houthavens	-	0.40	-	-	-	-0.22	Zuidas	-	0.24	-	-	-	-
	IJburg Oost	-0.09	-	-	-	-	-	P&R Bos&L.	0.08	0.29	0.19	-	-	-
	Middenmeer	-	-	0.08	-	-	-	P&R Olymp.	-	0.23	-0.06	-0.08	0.43	-
	Nieuwmarkt	-	-	-	-	-0.19	-	P&R ArenA	0.07	0.09	-	-	0.04	-0.05
	Noord. IJ. W.	-	-	-	-	-	0.01	P&R Sloterd.	-	-	0.52	-	0.44	0.84
	Omval/Overa.	0.02	-	-	-	-	-	P&R VUmc	-	-	8e-3	-	-	-
	Overtoomsev.	-0.02	-	-	-0.08	-	-	P&R Zeeburg	0.01	0.18	-	-	0.24	0.04
Level	Parking tariff	4.15	-13.1	-13.8	13.4	20.3	-11.2	COVID-19	-37.2	-59.1	-61.3	-50.5	-52.6	-61.2
shift	NSL	7.02	-2.47	-	-	-11.1	-15.1							

* Parking locations: Buikslotermeer (BUI), Burgwallen-Nieuwe Zijde (BUR), Zuidas (ZUI), Bijlmer Center (BIJ), P&R Bos en Lommer (PRB) and P&R Olympisch Stadion (PRO).
** The % change is per visitor to the event for the cultural, sports and meeting events.

The results emphasize that major changes, specifically the NSL, tariff increase, and the COVID-19 lockdown, have the most significant impact. When comparing the impact of the NSL to the tariff increase, it becomes clear that the most pronounced alterations in parking behavior in the center are linked to the tariff increase. These findings contribute to the existing literature, which has limited research comparing multiple measures using time series data.

Beyond the scope of this case study, we offer the following suggestions to parking policymakers: Firstly, it is crucial to recognize that these measures may not necessarily decrease overall parking in the city but could lead to a shift in parking behavior, often described as a "waterbed effect." Secondly, push factors, such as a tariff increase, seem to exert a more substantial influence on reducing parking in specific locations. Nevertheless, strategically combining these with pull factors, such as the introduction of a new metro

line, can serve as an effective approach to gradually mitigate parking in central areas, as illustrated in Figure 12.

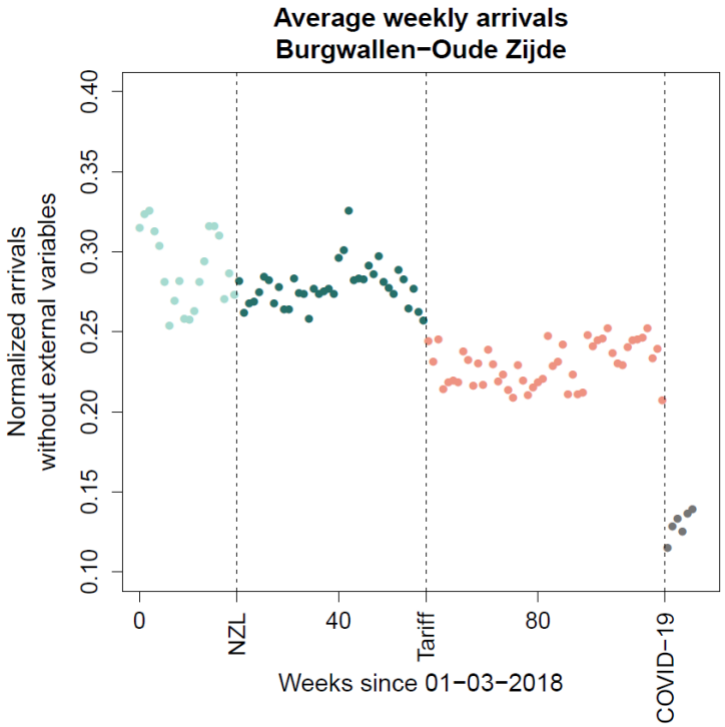

Figure 12. Impact of level shift attributes in Burgwallen-Oude Zijde

To further investigate the impact of the tariff increase in the city center, beyond its influence on parked cars, it is valuable to consider its potential effects on visitor numbers. Despite the policy changes, the total number of visitors per year continued to demonstrate a consistent upward linear trend until 2019, with no apparent alterations in monthly patterns. Over this period, visitor figures ascended from 19.8 million in 2017 to 20.9 million in 2018, and further to 21.5 million in 2019, of which around 53% comprised day visitors (Municipality of Amsterdam, 2023). Given this upward trend observed and the availability of only yearly data for day visitors, it becomes essential to delve into the more fine-grained nuances to study the effects on visitor numbers given the policy measures. Additionally, the COVID-19 pandemic between 2020 and 2022 led to a significant decline in visitor numbers, complicating long-term effect assessment. Expanding our research to include more detailed visitor metrics is crucial to fully understand the impact of the tariff increase. However, data scarcity within this timeframe, compounded by pandemic disruptions, highlights the need for further investigation.

5.3 Land-use implications

The reduction in on-street parking demand as an effect from the policy measures was a strategic initiative aimed at reshaping land-use dynamics. With the city's overarching goal of eliminating over 10 thousand parking spaces by 2025 in mind, the reduction in demand facilitated an annual strategy for on-street parking decommissioning. These vacated parking spaces were subsequently repurposed to serve alternative functions, as illustrated in Figure 13. This figure outlines the yearly decommissioning of parking

spaces alongside the alternative functions adopted at these locations, including redevelopment, elimination of parking spaces to relieve bridges and quays (notably in the Center where bridges and quays were becoming overloaded), installation of bicycle racks (predominantly in the South), housing construction (notably in Amsterdam Nieuw-West, an area characterized by its abundant public space), and the implementation of greening initiatives, safe crossings, and expanded pedestrian areas in central and western Amsterdam. Additionally, the repurposed spaces accommodated various other functions including waste management, shared mobility, coach stops, rainproofing, service facilities, bicycle infrastructure, and public transport infrastructure.

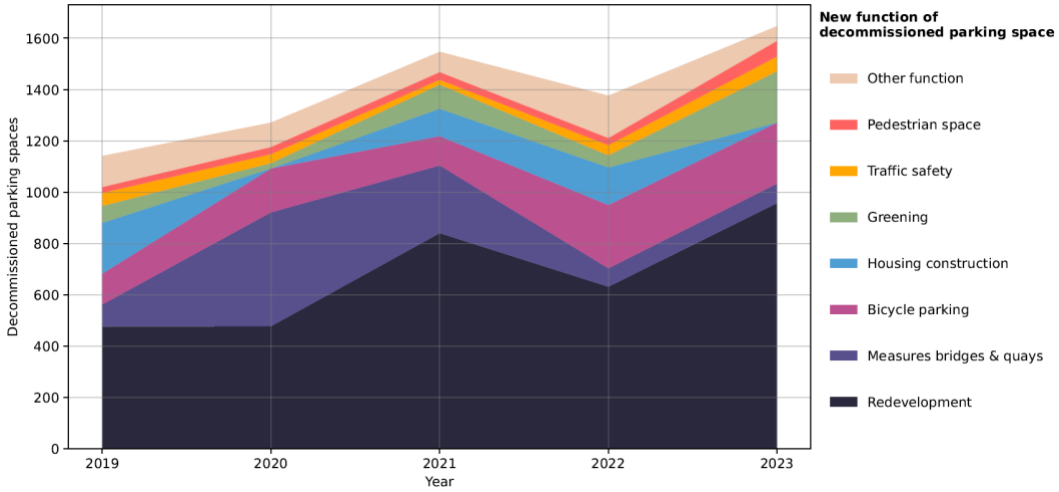

Figure 13. Land-use transformations of decommissioned parking spaces in Amsterdam, the Netherlands (Data collected from Amsterdam's Traffic and Public Space Department and the Car-Low program (Autoluw))

Moreover, current on-street parking spaces are shifted to two central Amsterdam parking garages, enabling city center parking without compromising public space on the streets. In 2023, the five-floor Vijzelgracht Parking Garage opened, providing 70 spaces for residents. In 2024, the underground Marnix Parking Garage opened, accommodating 800 parking spots.

Another noteworthy trend is the growing prevalence of off-streets commercial parking providers offering parking spaces at rates lower than those of street parking. This trend suggests a phenomenon of substitution, wherein parking spaces previously available on the streets are now accessible through these commercial entities, comparable to traditional public garages. Yet, due to ethical considerations, precise data on the number of parking spaces provided by these companies remains ambiguous. However, it is expected that the current total number of these facilities exceeds 175.

5.4 Application

To present the results as in Table 6 an interactive fashion a Decision Support System (DSS) called *ParkMotion* is developed. Keen (1980) defined a DSS as a "small-scale, interactive system designed to provide managers with flexible, responsive tools that act in effect as a staff assistant, to whom they can delegate more routine parts of their job." These systems do not replace a decision-maker's judgement, but instead provide access to information, models and reports and help to extend the decision maker's scope of

analysis. The DSS is built using the open-source framework Dash from the Plotly library in Python. The input to this DSS consists of the empirical hourly number of parking ticket transactions observed during the measurement period, along with the coefficients obtained from the ETSX model for each exogenous regressor.

The interface of the DSS is presented in Figure 14. Figure (a) visualizes the graphics of the "time series mode", which visualizes the number of observed transactions for a selected aggregation level, neighborhood/tariff zone, granularity and time period. The darker the color on the map, the higher the demand for parking ticket transactions on the given time period. From the selected time series clear decrease due to the start of the COVID-19 lockdown can be observed. Figure (b) visualizes the graphics of the "external variable mode". For each aggregation level and external variable, the percentage impact of the external variable per area can be analyzed. For instance, in many tariff zones the number of transactions has decreased by 10% until 80% in some locations as a result of the tariff change.

6 Conclusions and future studies

This paper employs time series and machine learning models to analyze parking demand and assess policy-induced changes in on-street and P&R demand in Amsterdam. Comparing Seasonal Naïve, SARIMAX, ETSX, and IMV-LSTM models, we find that incorporating external regressors enhances prediction accuracy. Notably, ETSX achieves the lowest RMSE and SMAPE values, making it the preferred model for investigating parking demand shifts. Notably, three major measures—parking tariff increase, the opening of the metro line NSL and the lockdown as a result of the pandemic—have significantly altered parking behavior in Amsterdam. As the tariff increase has led to strong decrease in more expensive central areas (until -22%), more motorists tend to park in peripheral areas and P&R locations (e.g., 86% more in P&R RAI). The opening of the metro line has caused an 81% increase in the neighborhood nearby the northernmost station of the line. In the east and P&R locations further from the NSL stations a decrease of until 77% is detected. The tariff change yields the most significant changes when compared to the opening of the metro line. Finally, the COVID-19 measure has caused a sharp decline in all locations, especially in P&R locations and business parks. The reduction in on-street parking demand, particularly due to the tariff increase, was part of a strategic initiative to reshape land-use dynamics. To date, over 7.1 thousand on-street parking spaces have been decommissioned, with locations repurposed for redevelopment, bicycle parking, and other functions. Additionally, two parking garages have been opened in the center to accommodate parking needs without intruding on-street space. Moreover, a notable trend is the increase in commercial off-street parking providers replacing previous on-street spots.

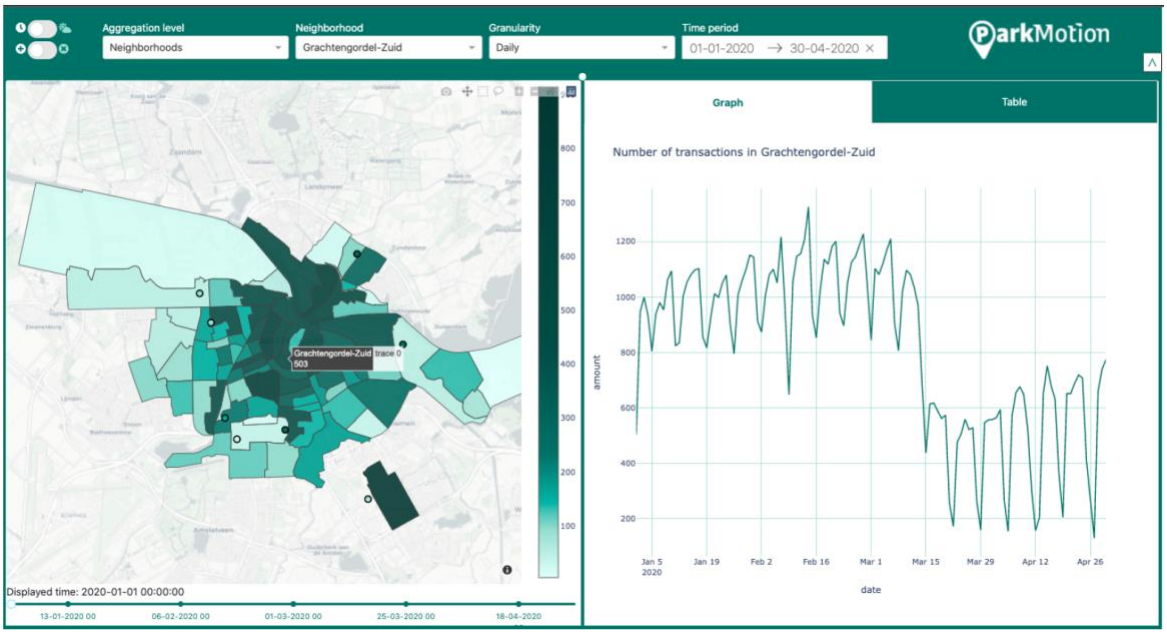

(a) Interface of the "time series mode"

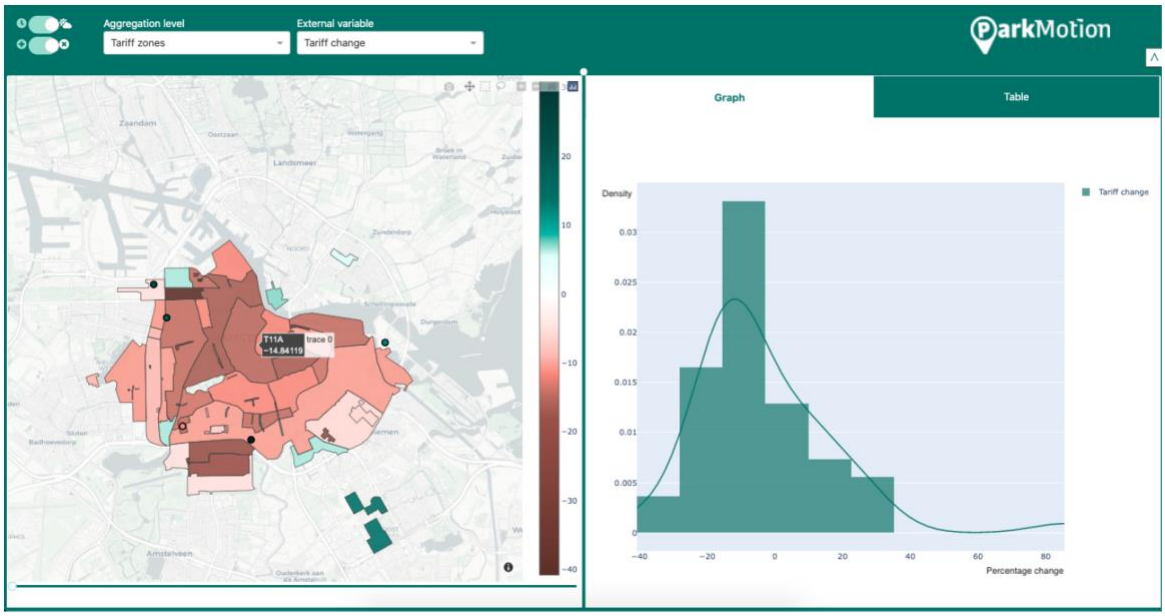

(b) Interface of the "external variable mode"

Figure 14. Interface of the Decision Support System

In addition to these measures, various factors such as weather conditions, scheduled events, holidays, vacations, and spatial attributes significantly influenced parking behavior in different locations. In terms of weather, parking demand tends to rise with lower temperatures and reduced sunshine duration, as well as higher precipitation and decreased horizontal visibility. This indicates that travelers are more inclined to use cars during adverse weather conditions, while reduced visibility may discourage driving.

Events also impacted a notable influence on parking demand, both near and far from the event venue. Holidays like New Year's Eve and King's Day decreased parking demand, likely due to the availability of free street parking in most districts on these occasions. Furthermore, parking arrivals not only impact neighboring areas but also extend to locations further within the city, considering the previous hour's trends. These findings are presented interactively via an application named *ParkMotion*, designed for use by the parking policymakers at the Municipality of Amsterdam.

In future studies the model performance of the IMV-LSTM model can be enhanced by better learning relationships between the different observations in the time series. This can be reached by including convolutional neural networks (CNN) in the LSTM cells. Because the model was computationally expensive, it was not possible to compare more hyperparameter combinations and external variable combinations. Optimization of the IMV-LSTM models can provide a means to explore the model parameter combinations in more detail. Another avenue for future research involves integrating visitor information to explore the impacts of the tariff change on the number of day visitors. This paper demonstrates the usefulness of external regressors in time series models: not only do they enhance model performance, but they also allow for the assessment of their impact on the target variable. Interpretable time series models with external regressors are a good example of bridging the gap between theoretical results from models and practical applications. Therefore, these models are well-suitable to provide empirical evidence for more intelligent policymaking.

Acknowledgments

This research has been conducted in the framework of the Impact Study North/Southline research theme "Mobility and Accessibility" hosted at CWI and funded by the Municipality of Amsterdam and the regional transportation authority of Amsterdam. We greatly appreciate the help of Marco van Leeuwen from the parking sector, who provided crucial insights into land-use, visitor information, and parking dynamics. Additionally, we express our gratitude to Barry Ubbels, Rutger Veldhuijzen van Zanten, and Machiel Kouwenberg from the regional transportation authority of Amsterdam (Vervoerregio Amsterdam) for their insightful perspectives on land-use dynamics. Lastly, we would like to express our appreciation to the three reviewers for their constructive feedback on an earlier version of this paper, which significantly improved its quality.

References

Akiba, T., Sano, S., Yanase, T., Ohta, T., & Koyama, M. (2019). Optuna: A next-generation hyperparameter optimization framework. *Proceedings of the 25th ACM SIGKDD International Conference on Knowledge Discovery & Data Mining*, 2623–2631.

Arjona, J., Linaresa, M., Casanovas-Garcia, J., & Vázqueza, J. J. (2020). Improving parking availability information using deep learning techniques. *Transportation Research Procedia*, *47*, 385–392.

Arnott, R., & Inci, E. (2006). An integrated model of downtown parking and traffic congestion. *Journal of Urban Economics*, *60*(3), 418–442.

Barter, P. A. (2011). *Parking Policy in Asian Cities*. Retrieved from https://www.adb.org/publications/parking-policy-asian-cities

Bisht, D. C. S., & Ram, M. (2021). *Recent advances in time series forecasting*. Boca Raton, FL: CRC Press.

Camero, A., Toutouh, J., Stolfi, D. H., & Alba, E. (2019). Evolutionary deep learning for car park occupancy prediction in smart cities. *Learning and Intelligent Optimization: 12th International Conference, LION 12, Kalamata, Greece, June 10–15, 2018, Revised Selected Papers 12*, 386–401.

Craney, T. A., & Surles, J. G. (2002). Model-dependent variance inflation factor cutoff values. *Quality Engineering*, *14*(3), 391–403.

Engel-Yan, J., Hollingworth, B., & Anderson, S. (2007). Will reducing parking standards lead to reductions in parking supply? Results of extensive commercial parking survey in Toronto, Canada. *Transportation Research Record*, *2010*(1), 102–110.

Fabusuyi, T., Hampshire, R. C., Hill, V. A., & Sasanuma, K. (2014). Decision analytics for parking availability in downtown Pittsburgh. *Interfaces*, *44*(3), 286–299.

Feng, N., Zhang, F., Lin, J., Zhai, J., & Du, X. (2019). Statistical analysis and prediction of parking behavior. *Network and Parallel Computing: 16th IFIP WG 10.3 International Conference, NPC 2019, Hohhot, China, August 23–24, 2019, Proceedings 16*, 93–104.

Fokker, E. S., Koch, T., & Dugundji, E. R. (2021). *Long-Term forecasting of off-street parking occupancy for smart cities*. Retrieved from https://doi.org/10.1177/03611981211036373

Fokker, E. S., Koch, T., van Leeuwen, M., & Dugundji, E. R. (2022). Short-term forecasting of off-street parking occupancy. *Transportation Research Record*, *2676*(1), 637–654.

Ghosal, S. S., Bani, A., Amrouss, A., & El Hallaoui, I. (2019). A deep learning approach to predict parking occupancy using cluster augmented learning method. *2019 International Conference on Data Mining Workshops (ICDMW)*, 581–586.

Guha, S., Mishra, N., Roy, G., & Schrijvers, O. (2016). Robust random cut forest-based anomaly detection on streams. *International Conference on Machine Learning*, 2712–2721.

Guo, T., Lin, T., & Antulov-Fantulin, N. (2019). Exploring interpretable LSTM neural networks over multi-variable data. *International Conference on Machine Learning*, 2494–2504.

Hochreiter, S., & Schmidhuber, J. (1997). Long short-term memory. *Neural Computation*, *9*(8), 1735–1780.

Hyndman, R. J., Koehler, A. B., Ord, J. K., & Snyder, R. D. (2008). *Forecasting with exponential smoothing: The state space approach*. Berlin: Springer Science & Business Media.

Inci, E. (2015). A review of the economics of parking. *Economics of Transportation*, *4*(1–2), 50–63.

Jakle, J. A., & Sculle, K. A. (2004). Introduction In *Lots of parking: Land use in a car culture*. Charlottesville, VA: University of Virginia Press.

Keen, P. G. W. (1980). *Decision support systems and managerial productivity analysis* (Issue CISR technical report No. 60 and Sloan W.P. No. 115680). Cambridge, MA: MIT.

Kelly, J. A., & Clinch, J. P. (2006). Influence of varied parking tariffs on parking occupancy levels by trip purpose. *Transport Policy*, *13*(6), 487–495.

Kirschner, F., & Lanzendorf, M. (2020). Parking management for promoting sustainable transport in urban neighborhoods. A review of existing policies and challenges from a German perspective. *Transport Reviews*, *40*(1), 54–75.

Kodransky, M., & Hermann, G. (2011). *Europe's parking u-turn: From accommodation to regulation.* New York: Institute for Transportation and Development Policy.

Liu, K. S., Gao, J., Wu, X., & Lin, S. (2018). On-street parking guidance with real-time sensing data for smart cities. *2018 15th Annual IEEE International Conference on Sensing, Communication, and Networking (SECON)*, 1–9.

Lu, E. H.-C., & Liao, C.-H. (2018). A parking occupancy prediction approach based on spatial and temporal analysis. *Intelligent Information and Database Systems: 10th Asian Conference, ACIIDS 2018, Dong Hoi City, Vietnam, March 19-21, 2018, Proceedings, Part I 10*, 500–509.

Makridakis, S., Wheelwright, S. C., & Hyndman, R. J. (2008). *Forecasting methods and applications* (3rd ed.). Hoboken, NJ: John Wiley & Sons. https://books.google.nl/books?id=nxt0CgAAQBAJ

Marsden, G. (2014). Parking policy. In *Parking issues and policies* (pp. 11–32). Bingley, UK: Emerald Group Publishing Limited.

Miller, T. (2019). Explanation in artificial intelligence: Insights from the social sciences. *Artificial Intelligence*, *267*, 1–38.

Mingardo, G., van Wee, B., & Rye, T. (2015). Urban parking policy in Europe: A conceptualization of past and possible future trends. *Transportation Research Part A: Policy and Practice*, *74*, 268–281.

Mukhija, V., & Shoup, D. (2006). Quantity versus quality in off-street parking requirements. *Journal of the American Planning Association*, *72*(3), 296–308.

Municipality of Amsterdam; Department of Traffic and Public Space. (2020). *Amsterdam maakt ruimte. Agenda Amsterdam autoluw*. Amsterdam: Municipality of Amsterdam, Department of Traffic and Public Space. https://www.amsterdam.nl/verkeer-vervoer/agenda-amsterdam-autoluw/

Pflügler, C., Köhn, T., Schreieck, M., Wiesche, M., & Krcmar, H. (2016). Predicting the availability of parking spaces with publicly available data. In H. C. Mayr & M. Pinzger (Eds.), *Infomatik 2016, Lecture notes in informatics* (pp. 361–374). Bonn, Germany: Gesellschaft für Informatik.

Provoost, J. C., Kamilaris, A., Wismans, L. J. J., van Der Drift, S. J., & van Keulen, M. (2020). Predicting parking occupancy via machine learning in the web of things. *Internet of Things*, *12*, 100301. http://www.sciencedirect.com/science/article/pii/

Richter, F., Di Martino, S., & Mattfeld, D. C. (2014). Temporal and spatial clustering for a parking prediction service. *2014 IEEE 26th International Conference on Tools with Artificial Intelligence*, 278–282.

Rong, Y., Xu, Z., Yan, R., & Ma, X. (2018). Du-parking: Spatio-temporal big data tells you real-time parking availability. *Proceedings of the 24th ACM SIGKDD International Conference on Knowledge Discovery & Data Mining*, 646–654.

Russell, S. J., & Norvig, P. (2016). *Artificial intelligence: A modern approach* (3rd ed.). London: Pearson Education, Inc.

Shoup, D. C. (2005). *High cost of free parking* (1st ed.). London: Routledge. https://doi.org/https://doi.org/10.4324/9781351179539

Shoup, D. C. (2006). Cruising for parking. *Transport Policy*, *13*(6), 479–486.

Taylor, E. J. (2020). Chapter 2 – Melbourne: Australia. In D. Pojani, J. Corcoran, N. Sipe, I. Mateo-Babiano & D. Stead (Eds), *Parking: An international perspective* (pp 15–35). Elsevier. https://doi.org/10.1016/C2017-0-02976-2

van Der Lof, M., & Bussink, B. (2019). *Amsterdamse thermometer van de openbare ruimte 2019*. Amsterdam: Municipality of Amsterdam, Department of Traffic and Public Space. https://openresearch.amsterdam/nl/page/87828/amsterdamse-thermometer-van-de-bereikbaarheid-2019

Wang, H., Li, R., Wang X.C, & Shang, P. (2020). Effect of on-street parking pricing policies on parking characteristics: A case study of Nanning. *Transportation Research Part A: Policy and Practice*, *137*, 65–78.

Welsh, G., & Bishop, G. (1995). *An introduction to the Kalman filter*. Chapel Hill, NC: University of North Carolina.

Zhang, F., Liu, Y., Feng, N., Yang, C., Zhai, J., Zhang, S., ..., & Du, X. (2021). Periodic weather-aware LSTM with event mechanism for parking behavior prediction. *IEEE Transactions on Knowledge and Data Engineering*, *34*(12), 5896–5909.